XXXVI Ibero-Latin American
Congress on Computational
Methods in Engineering
CILAMCE
Rio de Janeiro, 22-25 Nov 2015

NUMERICAL RESERVOIR SIMULATION OF SHALE GAS IN THE SLIP FLOW REGIME

Camila Lima Chung

Mayksoel Medeiros de Freitas

Grazione de Souza

Helio Pedro Amaral Souto

mila_chan@msn.com

mayksoel@iprj.uerj.br

gsouza@iprj.uerj.br

helio@iprj.uerj.br

Instituto Politécnico, Universidade do Estado do Rio de Janeiro

Rua Bonfim 25, Vila Amélia, 28625-570, Nova Friburgo, Rio de Janeiro, Brazil

Abstract. *Sometimes on gas flow in porous media the conventional Darcy's law cannot adequately describe the flow. An example is the slip phenomenon, named Klinkenberg's effect, in which rock permeability is a pressure function. Several recent works have been dedicated to incorporate slip phenomena using Knudsen's number, a dimensionless number that relates the mean-free-path of molecules (function of fluid properties) and a characteristic hydraulic radius (dependent of rock properties). In this work, in order to study slip flow in porous media, a numerical reservoir simulation code was developed for studying porous media flow in field scale, considering very low permeability gas reservoirs (shale gas) and production through horizontal wells. The physical-mathematical modeling considers three-dimensional, single-phase and isothermal gas flow. In order to determine the apparent gas permeability, the slippage effect is incorporated using a function of the Knudsen's number considering intrinsic properties such as permeability, porosity, tortuosity, rarefaction coefficient and the Klinkenberg's factor. The nonlinear partial differential equations are discretized by means of the finite-difference method along with an implicit approach. Different production scenarios were studied, varying properties of rock and fluid, in order to study the gas slip on the hydrocarbons recovery.*

Keywords: *Finite-difference method, Gas flow, Horizontal well, Klinkenberg's effect, Shale gas.*

1 INTRODUCTION

Bird et al. (2002) appointed that porous media are present in many mass transfer phenomena, including as example, catalysis, chromatography, membrane filtration, industrial processes and hydrocarbon's recovery. According to the authors, predicting porous media flow is a difficult task and there are several mechanisms of mass transport in porous media, such as viscous flow, surface diffusion, thermal transpiration and thermal diffusion. Moreover, particularly for gas flow in porous media, the authors discussed the slip flow phenomena, which occurs when the mean-free-path of molecular are comparable to pore dimensions.

In their study about low permeability sands, Florence et al. (2007) related that gas slippage occurs when the mean-free-path of the fluid molecules is not longer negligible compared to a hydraulic radius. Hence, gas molecules can slip on the porous media. As result, there is an apparent permeability for gas flow which is bigger than the absolute permeability for a liquid flow. In a discussion about non-Darcy flow, Aziz & Settari (1979) also considered the slip flow in porous media. They argued that the traditional Darcy's law, an expression for momentum balance in porous media flow, is valid for a Newtonian fluid, flow rates where high-velocity effects are absent and when there is not slip flow. About fluid slippage, authors cited that experimentally it was observed a minimum pressure gradient necessary to start flow.

Thus, it is worth noting that for gas flow in porous media there are situations in which the conventional Darcy's law cannot adequately describe the flow. Data from some formations appointed that permeability corrections considering slip phenomenon, named Klinkenberg's effect, can be relevant for low permeability reservoirs. In the traditional Klinkenberg's modeling (Ertekin et al., 2001), permeability is a pressure function and there is a number, the Klinkenberg's coefficient, specific for each porous media under analysis, in order to modeling the gas slippage. A more complete model for slip flow is based on the Knudsen's number, Kn, a dimensionless number that relates the mean-free-path of molecules, dependent on fluid properties, and a characteristic hydraulic radius, dependent on the rock properties.

Studies on gas flow in a wide range of Knudsen's number at low Mach's number were accomplished by Bestok & Karniadakis (1999), in order to obtain models for rarefied gas flows in pipes of smooth surface. They related that when the mean free-molecular-path is comparable to a characteristic geometric scale, gas flow cannot be studied based on the continuum assumption. In function of Knudsen's number, the authors related that continuum scale is adequate for $Kn \leq 10^{-3}$, slip flow occurs for $10^{-3} < Kn < 0.1$, a transition regime exists for $0.1 \leq Kn \leq 10$ and $Kn \geq 10$ indicates a free molecular flow. According to Swami et al. (2012), for shale gas reservois, slip and transition flows are two characteristic regimes.

In the context of porous media, Civan (2010 b) considered tight porous media in order to obtain a effective correlation to the apparent gas permeability, including different flow regimes in function of the Knudsen's number. This study presented a rigorous approach to take into account the effect of the characteristic parameters including, as example, porosity, intrinsic permeability, tortuosity, rarefaction coefficient and Klinkenberg's factor on the apparent gas permeability. Civan (2010 b) related that the correlation presented is more accurate than the suggested in previous works. Particular cases, as example, slip flow conditions, conducted to a simpler correlation, also presented.

An improved formulation involving mechanisms of retention and transport, considering shale gas reservoirs (very low permeability gas reservoirs), was considered by Civan et al.

(2011) in order to determine gas permeability and diffusivity. The model presented incorporated continuum, slip, transition and molecular flow in function of the Knudsen's number. According to the authors, the model proposed has adequate concordance to experimental results. The computation of apparent gas permeability was based on Civan (2010 b).

Li et al. (2014) studied tight and shale gas reservoirs, considering transient pressure responses. According to the authors, the Klinkenberg's coefficient, a parameter in the slip flow modeling, is not a constant for tight and shale gas reservoir. They studied apparent permeability like a Knudsen's number function and considered gas adsorption, frequently present in shale gas reservoirs, and also studied by Civan et al. (2011). Several works have been done considering slip flow phenomena in porous media (Wu et al., 1998; Chastanet et al., 2007; Hu et al., 2009; Civan, 2010 a; Wu et al., 2011; Ziarani & Aguilera, 2012; Hayek, 2015), especially because this effect can be present in unconventional reservoirs, formations increasingly studied, which require particular techniques of analysis and explotation.

For unconventional reservoirs explotation, aiming to enable or increase the production, horizontal wells (Fig. 1) have been utilized to augment the contact area between reservoir and well (Akgun, 2004). They are indicated for low-thickness reservoirs, low-permeability formations and naturally fractured reservoirs. Compared to vertical wells, productivity forecasts are more subject to uncertainty in the case of horizontal wells. This is due to the fact that flow regimes in a reservoir with a horizontal well are not so clearly identified as those for a vertical well (Chaudhry, 2003). This partially results from the fact that the nature of the flow is inherently three-dimensional (the radial symmetry observed in vertical wells does not occur in the same form for horizontal wells). Due to its importance for reservoir engineering applications, much research has been done considering horizontal wells (Al-Mohannadi, 2004; Al-Mohannadi et al., 2007; De Souza, 2013; De Souza et al., 2014; Shahbazi et al., 2015).

Hydraulic fracturing is also an alternative in order to enhance well production in unconventional reservoirs (Xie et al., 2014). For a hydraulic fractured horizontal well, fluid flows from the porous media to the horizontal well through an artificial fracture network. In some applications, hydraulic fractured horizontal wells are applied in naturally fractured reservoirs (NFRs). In these rock formations, there are permeability (k) and porosity (ϕ) fields with high contrasts caused by geological factors. A natural fracture is a planar discontinuity in reservoir rock due to deformation or diagenesis (chemical and physical changes after deposition) (Tiab & Donaldson, 2004).

For a certain class of simplified cases, as example, one-dimensional flow of slightly compressible fluid, there are analytic solutions available for porous media flow. However, for complex systems and more realistic flows, numerical simulation is a very important tool (Ertekin et al., 2001). Numerical solutions are considered for several problems including gas flow, for instance. In this case, governing partial differential equations for porous media flow are non-linear. This stems from the fluid properties dependency on pressure (Jmili et al., 2011; He & Durlofsky, 2013). Another non-linearity come from the so called non-Darcy effects, like the slip phenomena. Reservoir simulation studies are helpful for reservoir management and consequent increment in the hydrocarbon factor recovery. It is important to note that in the last decades a number of engineers and scientists have worked on the optimized recovery in unconventional hydrocarbons reserves, as example, shale gas. Indeed, shale gas reservoirs are increasingly becoming important players in the world energy matrix.

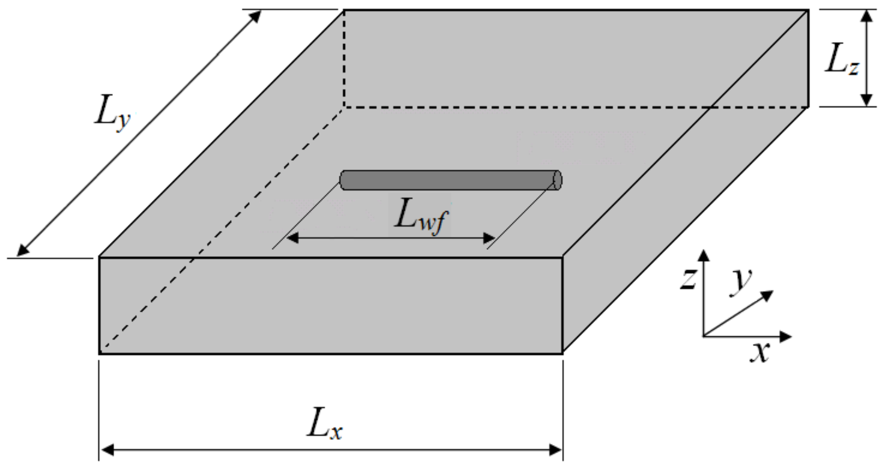

Figure 1: Representation of a reservoir and a horizontal well, of length L_{wf}, parallel to x- direction.

In this work, porous media flow in shale gas is studied considering the slip flow phenomena and production through horizontal well. In order to study this situation, a three-dimensional field scale reservoir simulator was developed using Cartesian coordinates and a classical finite-difference approach. The physical-mathematical modeling considers single-phase and isothermal gas flow, without adsorption effects, which can be present in certain applications involving shale gas reservoirs. Water presence in shale gas reservoirs influences slippage phenomena (slip factor decreases with the increase of the water saturation). Hydraulic and natural fractures are not also considered in this study. A non-linear partial differential equation for unknown pressure is numerically solved using the preconditioned conjugate gradient method. Moreover, a grid refinement is applied to better capture flow characteristics near the horizontal well. The main objective is accomplished by simulating production scenarios and discussing combined effects of rock and fluid properties on the Knudsen's number, and hence, on the slip flow phenomenon. Motivations for this research are the increasing production and consumption of natural gas and the explotation of unconventional hydrocarbons reserves.

2 PHYSICAL-MATHEMATICAL MODELING

In porous media flow, a partial differential equation for unknown pressure can be obtained from a fundamental set of governing equations composed by mass conservation, an expression for momentum balance and an equation of state. Typically, flow in porous media is modeled using the well-known Darcy's law, that predicts a linear relationship between the superficial velocity and the pressure gradient. However, in some cases, as example, slippage effects, can lead to deviations from the predicted values obtained with the original Darcy's law. Then, generally, a modified Darcy's law is written in order to incorporate non-Darcy flow effects.

2.1 Governing Equations for Porous Media Flow

In the following, a pressure equation for porous media flow will be obtained using these equations and considering as assumptions: heterogeneous rock formation, constant intrinsic permeabilities, low and constant rock compressibility, Newtonian fluid, dry gas reservoir, fluid of constant composition, single-phase isothermal flow and slip phenomena.

First of all, mass conservation for porous media flow can be written as

$$\frac{\partial}{\partial t}(\phi\rho) + \nabla\cdot(\rho\mathbf{v}) - \frac{q_m}{V_b} = 0, \tag{1}$$

where $\mathbf{v}$ is the superficial fluid velocity, ρ represents density, q_m is a source term and V_b indicates the bulk volume.

For a real gas flow, density is a non-linear function of pressure and temperature given by

$$\rho = \frac{pM}{ZRT}, \tag{2}$$

where M is the molecular gas weight, Z represents real gas deviation factor (dependent on pressure, temperature and on M), R is the universal gas constant and T indicates temperature. Equation (2) is used along with the formation-value-factor, B,

$$B = \frac{V}{V_{sc}} = \frac{\rho_{sc}}{\rho} = \frac{p_{sc}TZ}{T_{sc}p}, \tag{3}$$

where V is fluid volume at reservoir conditions, V_{sc} is fluid volume at standard conditions and p_{sc} and T_{sc} are pressure and temperature at standard conditions, respectively.

Generally, the traditional Darcy's law is applied in order to express the conservation of momentum in porous media flow

$$\mathbf{v} = -\frac{\mathbf{k}}{\mu}[\nabla p - \rho g\nabla D], \tag{4}$$

where $\mathbf{k}$ is the permeability, μ the fluid viscosity, p the pressure, ∇D is the depth gradient and g is the gravity acceleration. For gas flow, viscosity must be modeled as a function of pressure, temperature and of molecular gas weight.

The slip or Klinkenberg's effect occurs in gas flow under certain set of conditions (as example, low permeability) and results in an increment of effective permeability compared to the flow of liquids. Darcy's law can be modified to take into account slip flow,

$$\mathbf{v} = -\left(1 + \frac{b_k}{p}\right)\frac{\mathbf{k}_\infty}{\mu}[\nabla p - \rho g\nabla D] \tag{5}$$

in which b_k is the Klinkenberg's coefficient and $\mathbf{k}_\infty$ is the intrinsic permeability of the porous media (measured for single phase liquid flow). In many applications, b_k is considered a constant. However, an apparent permeability can be aldo modeled in function of the Knudsen's number (Civan et al., 2011),

$$\mathbf{k}_{app} = \mathbf{k}_\infty(1 + \alpha Kn)\left(1 + \frac{4Kn}{1 - bKn}\right) \tag{6}$$

where α is a rarefaction coefficient (dimensionless), b indicates a slip coefficient and Kn represents the Knudsen's number. Eq. (6) incorporates different flow regimes in one single representation (continuum, slip, transition and free molecular flow regimes). Under slip conditions, Civan (2010 b) considered $\alpha = 0$ and $b = -1$, and, therefore,

$$\mathbf{k}_{app} = \mathbf{k}_{\infty} \left(1 + \frac{4Kn}{1+Kn}\right). \tag{7}$$

As related by Florence et al. (2007), for $Kn << 1$, it is possible writing this following approximation

$$\mathbf{k}_{app} \approx \mathbf{k}_{\infty} (1 + 4Kn) \tag{8}$$

The Knudsen number measures the ratio of the free molecular path, λ, to a representative path, R_h, i.e.,

$$Kn = \frac{\lambda}{R_h} \tag{9}$$

where R_h is an measurement of the mean hydraulics radius of flow tubes formed in the porous media flow.

The free molecular path is computed as

$$\lambda = \frac{\mu}{p}\frac{\pi RT}{2M} \tag{10}$$

and, for the mean hydraulics radius,

$$R_h = 2\sqrt{2\tau}\sqrt{\frac{k_{\infty}}{\phi}} \tag{11}$$

where τ is the tortuosity of the porous media (Civan, 2010 b). One can obtain from Eqs. (10) and (11)

$$Kn = \frac{\mu}{4p}\sqrt{\frac{\pi RT\phi}{M\tau k_{\infty}}}. \tag{12}$$

Hereafter, in order to modeling permeability, it will be considered an apparent permeability given by Eq. (7).

2.2 Non-Linear Hydraulic Diffusivity Equation

In order to obtain a pressure equation, mass balance equation, real gas equation of state and a modified Darcy's law are considered as fundamental equations. First of all, a modified Darcy's law is written using $\mathbf{k}_{app}$

$$\mathbf{v} = -\frac{\mathbf{k}_{app}}{\mu}[\nabla p - \rho g \nabla D]. \tag{13}$$

Replacing Eq. (13) in Eq. (1), one can obtain

$$\frac{\partial}{\partial t}(\phi\rho) - \nabla \cdot \left[\frac{\rho \mathbf{k}_{app}}{\mu}(\nabla p - \rho g \nabla D)\right] - \frac{q_m}{V_b} = 0. \tag{14}$$

Now, applying Eq. (3) in Eq. (14), multiplying by V_b and using $q_m = q_{sc}\rho_{sc}$ it is possible to write

$$V_b \frac{\partial}{\partial t}\left(\frac{\phi}{B}\right) - V_b \nabla \cdot \left[\frac{\mathbf{k}_{app}}{B\mu}(\nabla p - \rho g \nabla D)\right] - q_{sc} = 0. \tag{15}$$

Then, considering the following correlation for porosity variation (Ertekin et al., 2001)

$$\phi = \phi^0 \left[1 + c_\phi \left(p - p^0\right)\right], \tag{16}$$

where ϕ^0 and p^0 are porosity and pressure in a reference condition, respectively, and c_ϕ is the rock compressibility, yield (Ertekin et al., 2001)

$$V_b \frac{\partial}{\partial t}\left(\frac{\phi}{B}\right) = \Gamma \frac{\partial p}{\partial t}. \tag{17}$$

where

$$\Gamma = V_b \left[\frac{\phi_0 c_\phi}{B} + \phi \frac{\partial}{\partial p}\left(\frac{1}{B}\right)\right]. \tag{18}$$

From Eq. (17), Eq. (15) is rewritten as

$$\Gamma \frac{\partial p}{\partial t} - V_b \nabla \cdot \left[\frac{\mathbf{k}_{app}}{B\mu}\nabla p\right] + \Gamma_G - q_{sc} = 0, \tag{19}$$

where $\Gamma_G = V_b G$ and G includes gravitational effects.

We use q_{sc} to include wellbore pressure, p_{wf}, in Eq. (19) by the equation

$$q_{sc} = -J_w(p - p_{wf}) \tag{20}$$

where J_w is the Productivity Index (PI). J_w is a function of a set of parameters, as example, fluid, rock and geometric properties. There are many different expressions that can be applied for computation of PI, depending on reservoir, fluid, wellbore and flow characteristics (Dumkwu et al., 2012). In this work, an expression used by Al-Mohannadi (2004)for non-Darcy flow related to inertial effects was adapted and used in order to compute of PI. Well-reservoir coupling is accomplished using Eq. (20) and, then, wellbore pressure can be estimated even using rectangular coordinates for the reservoir representation.

Replacing Eq. (20) in Eq. (19) we get

$$\Gamma \frac{\partial p}{\partial t} - V_b \nabla \cdot \left[\frac{\mathbf{k}_{app}}{B\mu}\nabla p\right] + J_w(p - p_{wf}) + \Gamma_G = 0. \tag{21}$$

Equation (21) has the form of hydraulic diffusivity equation, a non-linear partial differential equation, where the dependent variable is the gas pressure.

Considering Cartesian coordinates, initial condition for pressure is given by

$$p(x, y, z, t = 0) = p_{init}(z), \tag{22}$$

where p_{init} is a function of z. Generally an initial pressure, P_i, is given at a datum level depth and, based on hydrostatic gradient, initial pressure distribution is computed for the porous media.

External boundary conditions, for no-flow boundaries (a sealed reservoir) are set as

$$\left(\frac{\partial p}{\partial x}\right)_{x=0,L_x} = \left(\frac{\partial p}{\partial y}\right)_{y=0,L_y} = \left(\frac{\partial p}{\partial z}\right)_{z=0,L_z} = 0, \tag{23}$$

where L_x, L_y and L_z are reservoir lengths in x-, y- and z- directions, respectively. Finally, internal boundary condition is applied using the well rate production prescribed, Q_{sc}, which is equal to the summation of q_{sc} for the cells where there is a part of the horizontal well. If the flow rate is fixed, wellbore pressure is variable. Instead, if the wellbore pressure is specified, the well flow rate is an unknown.

3 NUMERICAL SOLUTION

3.1 Discretization of the Hydraulic Diffusivity Equation

Finite Difference Method (FDM) (Ertekin et al., 2001) is applied on the discretization of the Eqs. (21)–(23). Figure 2 shows a representation of a discretized reservoir using three-dimensional Cartesian coordinates. In the following, integer indexes i, j and k indicate cell centers along x-, y- and z- directions, respectively. A fractional index, as $i \pm 1/2, j, k$, indicates a cell boundary.

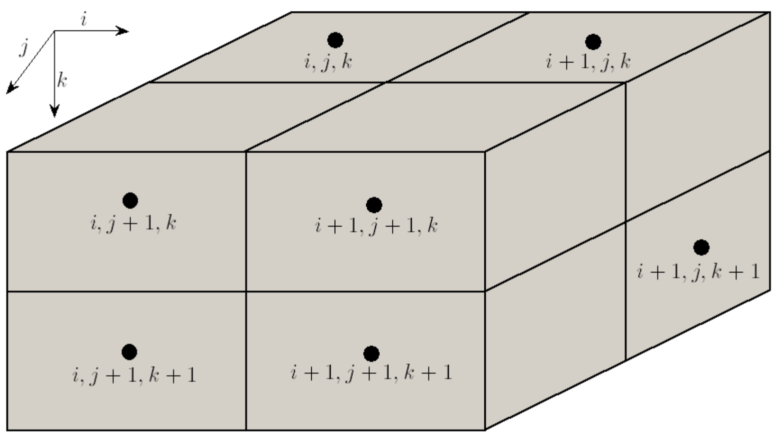

Figure 2: Finite difference discretization using Cartesian coordinates and centered blocks. Integer indexes indicate cell centers.

Considering an anisotropic medium,

$$\mathbf{k}_{app} = \begin{bmatrix} k_{app,x} & 0 & 0 \\ 0 & k_{app,y} & 0 \\ 0 & 0 & k_{app,z} \end{bmatrix} \tag{24}$$

and, thus, Eq. (21) can be rewritten as

$$\Gamma\frac{\partial p}{\partial t} - \frac{\partial}{\partial x}\left(\frac{k_{app,x}A_x}{B\mu}\frac{\partial p}{\partial x}\right)\Delta x - \frac{\partial}{\partial y}\left(\frac{k_{app,y}A_y}{B\mu}\frac{\partial p}{\partial y}\right)\Delta y - \frac{\partial}{\partial z}\left(\frac{k_{app,z}A_z}{B\mu}\frac{\partial p}{\partial z}\right)\Delta z$$
$$+J_w(p - p_{wf}) = -\Gamma_G, \tag{25}$$

where $V_b = \Delta x\Delta y\Delta z$, $A_x = \Delta y\Delta z$, $A_y = \Delta x\Delta y$ and $A_z = \Delta x\Delta y$.

Using a central difference approximation for centered blocks (Ertekin et al., 2001), we have

$$\frac{\partial}{\partial x}\left(\frac{k_{app,x}A_x}{B\mu}\frac{\partial p}{\partial x}\right)^{n+1}_{i,j,k} \approx \frac{1}{\Delta x_{i,j,k}}\left[\left(\frac{k_{app,x}A_x}{B\mu}\frac{\partial p}{\partial x}\right)_{i+\frac{1}{2},j,k} - \left(\frac{k_{app,x}A_x}{B\mu}\frac{\partial p}{\partial x}\right)_{i-\frac{1}{2},j,k}\right]^{n+1}, \tag{26}$$

where $\Delta x_{i,j,k}$ is the grid spacing in x- direction, $n+1$ represents the temporal level in which pressures are computed and n indicates a time level where pressure is known. Then, using once again central differences to approximate spatial pressure derivatives

$$\left(\frac{\partial p}{\partial x}\right)^{n+1}_{i+\frac{1}{2},j,k} \approx \frac{p^{n+1}_{i+1,j,k} - p^{n+1}_{i,j,k}}{\Delta x_{i+\frac{1}{2},j,k}} \quad \text{and} \quad \left(\frac{\partial p}{\partial x}\right)^{n+1}_{i-\frac{1}{2},j,k} \approx \frac{p^{n+1}_{i,j,k} - p^{n+1}_{i-1,j,k}}{\Delta x_{i-\frac{1}{2},j,k}}. \tag{27}$$

where $\Delta x_{i\pm 1/2,j,k}$ is the distance between cell centers numbered by i and $i \pm 1$. Similar forms can be obtained for y- and z- coordinates.

Now, transmissibility in x- direction is computed as

$$T^{n+1}_{x,i\pm\frac{1}{2},j,k} = \left(\frac{k_{app,x}A_x}{B\mu\Delta x}\right)^{n+1}_{i\pm\frac{1}{2},j,k} \tag{28}$$

where an harmonic average is applied to determine transmissibility at $i \pm 1/2, j, k$ from the known values in i, j, k and $i+1, j, k$. Analogous expressions also can be determined for y- and z- directions.

Finally, it is possible to get the final discretized form for Eq. (25)

$$\frac{\Gamma^{n+1}_{i,j,k}}{\Delta t}\left(p^{n+1}_{i,j,k} - p^{n}_{i,j,k}\right) - T^{n+1}_{x,i+\frac{1}{2},j,k}\left(p^{n+1}_{i+1,j,k} - p^{n+1}_{i,j,k}\right) - T^{n+1}_{x,i-\frac{1}{2},j,k}\left(p^{n+1}_{i-1,j,k} - p^{n+1}_{i,j,k}\right)$$
$$-T^{n+1}_{y,i,j+\frac{1}{2},k}\left(p^{n+1}_{i,j+1,k} - p^{n+1}_{i,j,k}\right) - T^{n+1}_{y,i,j-\frac{1}{2},k}\left(p^{n+1}_{i,j-1,k} - p^{n+1}_{i,j,k}\right)$$
$$-T^{n+1}_{z,i,j,k+\frac{1}{2}}\left(p^{n+1}_{i,j,k+1} - p^{n+1}_{i,j,k}\right) - T^{n+1}_{z,i,j,k-\frac{1}{2}}\left(p^{n+1}_{i,j,k-1} - p^{n+1}_{i,j,k}\right)$$
$$-J^{n+1}_{w,i,j,k}\left(p^{n+1}_{wf,i,j,k} - p^{n+1}_{i,j,k}\right) = -\left(\Gamma_G\right)^{n+1}_{i,j,k} \tag{29}$$

where a backward Euler approximation was used

$$\left(\frac{\partial p}{\partial t}\right)^{n+1}_{i,j,k} \approx \frac{p^{n+1}_{i,j,k} - p^{n}_{i,j,k}}{\Delta t} \tag{30}$$

and

$$\Gamma^{n+1}_{i,j,k} = V_{b,i,j,k}\left\{\frac{\phi^0 c_\phi}{B^{n+1}} + \frac{\phi^n}{B^n}\left[\frac{(B^n/B^{n+1}) - 1}{p^{n+1} - p^n}\right]\right\}_{i,j,k}. \tag{31}$$

A grid refinement is used in order to better represent the region near the horizontal well. For example, for a well placed normal on yz plane, grid spacing in y- direction, $\Delta y_{i,j,k}$, and in z-direction, $\Delta z_{i,j,k}$, are smaller near the cells that hosting the horizontal well. Considering indexes i, j and k as presented in Fig. 2 and used in the discretization, Fig. 3 displays a representation of grid refinement around the horizontal well localization. Δy_w and Δz_w are chosen for cells where the well is placed. For others cells, $\Delta y_{i,j,k}$ and $\Delta z_{i,j,k}$ are small near the well, and they increase at given rate as well as the cells are far from the horizontal well.

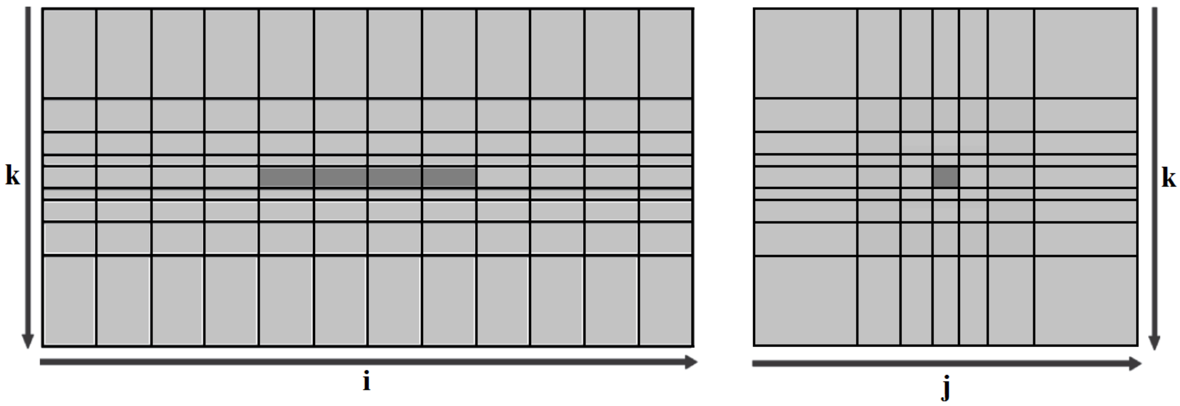

Figure 3: Grid refinement in order to better represent flow near horizontal well. In this case, the horizontal well is normal to yz -plane. On the left, xz -plane, and on the right, yz -plane. Cells that are hosting the horizontal well are in dark gray color.

3.2 Numerical Solution for Unknown Pressure

An implicit formulation applied to Eq. (25) yielded to Eq. (29). Written for each cell, Eq. (29) leads to a set of non-linear algebraic equations in terms of the unknown pressure. In order to use solution techniques for systems of linear equations, we must linearize the algebraic equations for pressures. Considering a simple iteration for transmissibility terms (Ertekin et al., 2001),

$$T^{n+1}_{x,i\pm\frac{1}{2},j,k} \cong T^{n+1,v}_{x,i\pm\frac{1}{2},j,k} = \left(\frac{k_{app,x}A_x}{B\mu\Delta x}\right)^{n+1,v}_{i\pm\frac{1}{2},j,k}, \tag{32}$$

Eq. (29) can be written as

$$\begin{aligned}
&\left(\Gamma^{n+1,v}_{i,j,k}/\Delta t\right)\left(p^{n+1,v+1}_{i,j,k} - p^{n}_{i,j,k}\right) - J^{n+1,v}_{w,i,j,k}\left(p^{n+1,v+1}_{wf,i,j,k} - p^{n+1,v+1}_{i,j,k}\right)\\
&-T^{n+1,v}_{x,i+\frac{1}{2},j,k}\left(p^{n+1,v+1}_{i+1,j,k} - p^{n+1,v+1}_{i,j,k}\right) - T^{n+1,v}_{x,i-\frac{1}{2},j,k}\left(p^{n+1,v+1}_{i-1,j,k} - p^{n+1,v+1}_{i,j,k}\right)\\
&-T^{n+1,v}_{y,i,j+\frac{1}{2},k}\left(p^{n+1,v+1}_{i,j+1,k} - p^{n+1,v+1}_{i,j,k}\right) - T^{n+1,v}_{y,i,j-\frac{1}{2},k}\left(p^{n+1,v+1}_{i,j-1,k} - p^{n+1,v+1}_{i,j,k}\right)\\
&-T^{n+1,v}_{z,i,j,k+\frac{1}{2}}\left(p^{n+1,v+1}_{i,j,k+1} - p^{n+1,v+1}_{i,j,k}\right) - T^{n+1,v}_{z,i,j,k-\frac{1}{2}}\left(p^{n+1,v+1}_{i,j,k-1} - p^{n+1,v+1}_{i,j,k}\right) = -\left(\Gamma_G\right)^{n+1,v}_{i,j,k}.
\end{aligned} \tag{33}$$

where iterative levels are indicated by v (known values) and $v+1$ (unknown values). The same procedure is used for $\Gamma_{i,j,k}$ and J_w terms.

To describe a well-reservoir coupling for a single phase flow, it is necessary an equation for the well flow rate and calculate J_w. Here, only horizontal wells are considered, neglecting frictional and convective effects inside the well. Total well flow rate, Q_{sc}, must be equal to gas flow summation from all cells trespassing the well, thus,

$$Q_{sc} = -\sum_{i=W1}^{i=W2} J_{w,i,j,k}^{n+1,v} \left[p_{i,j,k}^{n+1,v+1} - (p_{wf})_{i,j,k}^{n+1,v+1} \right] \tag{34}$$

for a well that trespassing layers along with x- direction, from cell numebered by $W1, j, k$ to $W2, j, k$. A reference position, in $W1, j, k$, is chosen in order to computing wellbore pressure.

For J_w we use

$$J_{w,i,j,k}^{n+1,v} = \left\{ \frac{2\pi\sqrt{k_{app,z}k_{app,y}}}{\mu B} \frac{\Delta x}{\left[1 - (r_w/r_{eq})^2\right] \ln\left(r_{eq}/r_w\right)} \right\}_{i,j,k} \tag{35}$$

and

$$r_{eq,i,j,k}^{n+1,v} = \sqrt{\frac{(\Delta z \Delta y)_{i,j,k}}{\pi}} \, \exp\left(-0.5\right). \tag{36}$$

where r_{eq} is the equivalent radius (Peaceman, 1983) and r_w is the wellbore radius. To taking into account the non-Darcy flow effects, apparent permeabilities are used in order to determine J_w and r_{eq} in Eq. (35), as applied by Al-Mohannadi (2004), but for inertial effects.

The set composed by Eq. (33) and Eq. (34) forms a system of equations for reservoir and wellbore pressures. The resulting system of linearized equations is solved using an approximate factorization technique. This technique has the capacity to deal with practical reservoir simulations, in which heterogeneity is present and, due to its scale, may impact some characteristics of the coefficient matrix (matrix conditioning). Here, the pre-conditioning conjugate-gradient method (PCG) was employed to solve the algebraic system of equations, using a diagonal preconditioner (Ertekin et al., 2001; Saad, 2003). Considering the iterative procedure, the numerical solution is achieved when

$$max \left| \chi^{n+1,v+1} - \chi^{n+1,v} \right| < tol \tag{37}$$

where χ represents reservoir and wellbore pressures and tol is a numerical tolerance. A nested iteration procedure (Ertekin et al., 2001) is used: in the inner iteration, PCG is applied in order to solve pressures and, in the outer iteration, transmissibilities are updated.

Finally, the numerical solution algorithm can be described by the following stages:

- Step 1: At time t, to advance Δt, estimate the unknown pressure values;
- Step 2: Until convergence:

  – Evaluate fluid and rock properties for grid cells and boundaries;

  – Evaluate the coefficients (as transmissibilities, J_w and Γ) for the system of equations;

  – Solve the system of equations for pressure using PCG method (Saad, 2003).

  – Verify convergence:

→ if tolerance was reached, update pressure values, $t = t + \Delta t$, go to Step 3;

→ else, return to Step 2.

- Step 3: if maximum time (t_{max}) was reached, Stop, else, return to Step 1.

4 NUMERICAL RESULTS

Results were obtained using the previously discussed methodology, considering numerical experiments for constant well production rate. In all numerical simulations, Lee et al. (1966) and Dranchuk & Abou-Kassem (1975) correlations for viscosity and real gas deviation factor were applied, respectively. Table 1 summarizes default data for all reservoir simulations. P_i is the pressure at the reservoir top, Q_{sc} is the wellbore production rate at standard m^3 per day and n_x, n_y and n_z are the numbers of cells in x-, y- and z-directions, respectively. The symbol n_w indicates the number of cells used to represent the well along with x- direction. $\Delta y_{i,j,k}$ and $\Delta z_{i,j,k}$ increase at rate of 1.5 as well as the cells are far from Δy_w and Δz_w related to the horizontal well placement. For all simulations, there was a computation of Kn in order to certify that only continuum and slip flows ocurried (behaviour verified in all tests).

Table 1: Default data used in all simulations.

Parameter	Value	Parameter	Value	Parameter	Value
p_{sc} (Pa)	1.0115×10^5	T_{sc} (K)	288.71	M (kg/kg-mol)	17.376
p^0 (Pa)	3.4474×10^7	τ	1.0	ϕ_0	0.05
P_i (Pa)	3.4474×10^7	T (K)	338.71	r_w (m)	0.0762
c_ϕ (Pa^{-1})	4.3511×10^{-10}	t_{max} (days)	365.0	ϕ_{init}	0.05
Q_{sc} (std m^3/day)	-2.864×10^3	n_x	48	L_{wf} (m)	609.6
$k_x = k_y = k_z$ (m^2)	9.8692×10^{-19}	n_y	49	L_z (m)	67.06
$L_x = L_y$ (m)	1.829×10^3	n_z	33	n_w	16

The numerical results were validated by comparing to the results from De Souza et al. (2014) for a porous media flow using data from Table 1, considering Darcy's law and without wellbore effects (discussed by De Souza et al. (2014)). It should be noted that De Souza's simulator had their results compared with the commercial simulator IMEX (Computational Modeling Group, 2009) and a good agreement was obtained. The results for the comparison are depicted in Fig. 4 and our results match very well with those from De Souza et al. (2014).

Table 2 shows data for a grid refinement study and Fig. 5 includes a plot of $p_{wf} \times \log t$ for different numerical grids, considering slip flow phenomenon. For the transient regime, a characteristic slope is obtained and there is evidence of numerical convergence as the grid is refined. It is worth to note that external boundary effects on pressure drop were detected (for the same time) for all grids and the pseudo-permanent regime starts at the same time, as expected.

Still with reference to Fig. 5, it is possible to note the existence of a plateau for all curves and short times. However, the extent of this plateau is dependent on the mesh size, so that the

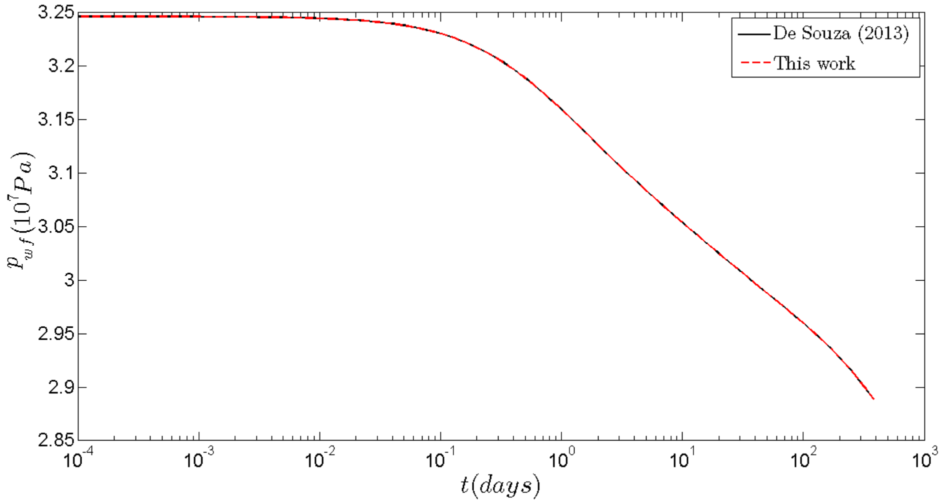

Figure 4: Study of validation.

Table 2: Grids for refinement study.

Grid	n_x	n_y	n_z	n_w	$\Delta y_w = \Delta z_w$ (m)
1	12	13	5	4	12.192
2	24	25	9	8	6.096
3	48	49	17	16	3.048
4	96	97	33	32	1.524

smaller plateau is associated with the finer grid. This is a numerical artifact well known in the literature, and it is due to the model of well-reservoir coupling (Peaceman, 1983). However, numerical results at early times can be improved by some specific techniques (Dumkwu et al., 2012, Al-Mohannadi et al., 2007), but the focus of this work was on transient and pseudo-permanent regimes in porous media. Thus, considering results after 1 day fo gas production, Grid 3 was chosen to be used in the numerical simulations.

Figure 6 shows the pressure drop versus time curves obtained using Darcy's law and the slip flow model for the same reservoir and production conditions. After the 365 days, pressure drop obtained using the modified Darcy's law is of approximately 90% of the related to the Darcy's law. This result confirms the importance of using models that take into account slippage effects in shale gas reservoirs.

A critical parameter that influences on the numerical artifact related to the well-reservoir coupling technique applied and on the Knudsen's number is the intrinsic permeability. Different values of k_∞ were tested for slip flow modeling and results are presented in Figs. 7. As expected, slip effects are more significant for low values of k_∞, due to the increment in Kn.

The numerical artifact associated to well-reservoir coupling has bigger influence also for lower permeability. Rock permeability also influences the time related to boundary effects, as shown (for higher permeabilities, boundary effects occur earlier). Porosity and tortuosity also were varied from default data and results are displayed in Figs. 8 and 9, respectively. Results are

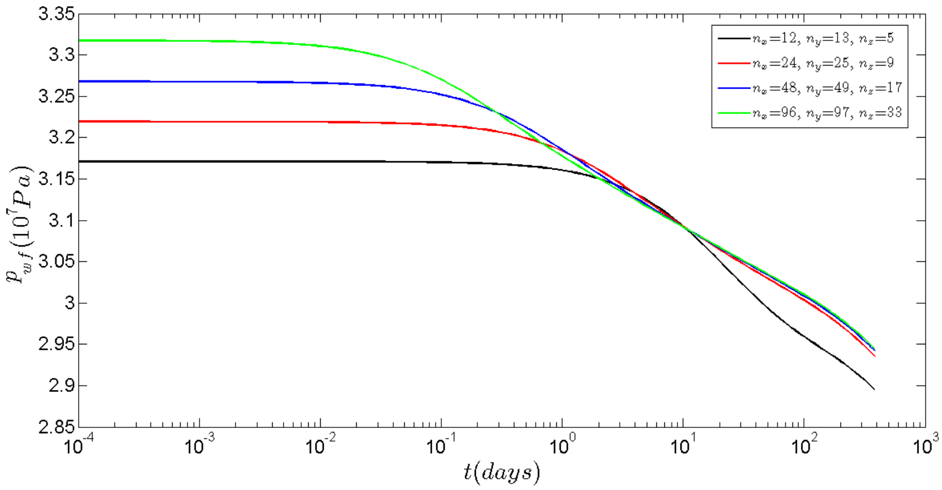

Figure 5: Grif refinement study.

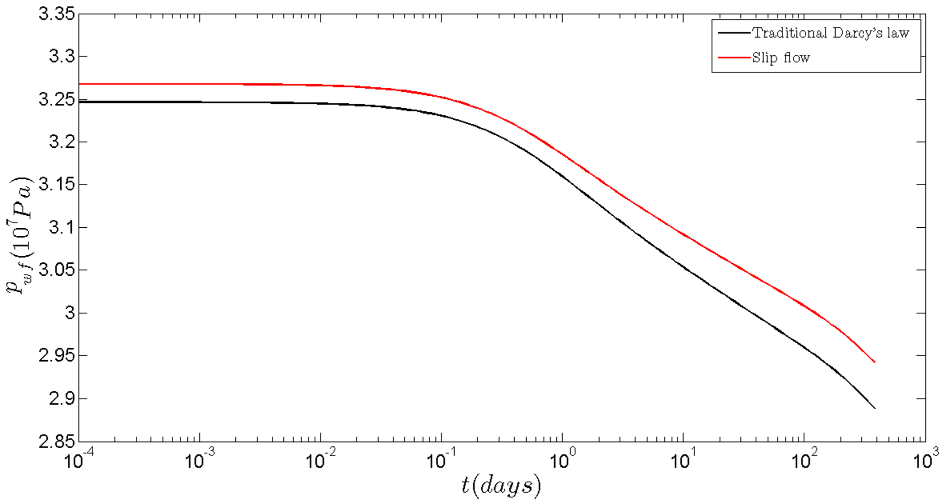

Figure 6: Results for Darcy's law and slip flow.

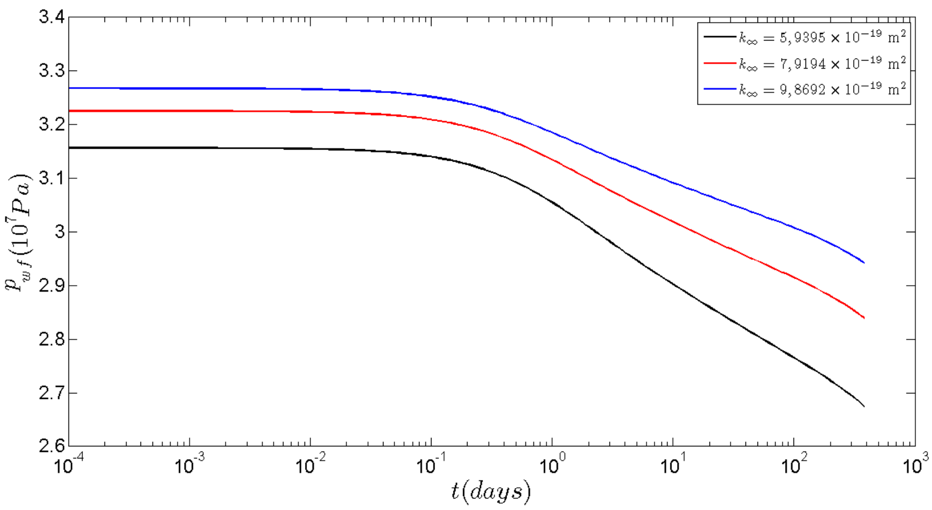

Figure 7: Results for different intrinsic permeabilities.

adequate to the physical modeling about slippage, which is more significant for bigger porosity and lower tortuosity. Remembering, porosity influences the time related to boundary effects, what was verified (for lower porosity, boundary effects occur earlier).

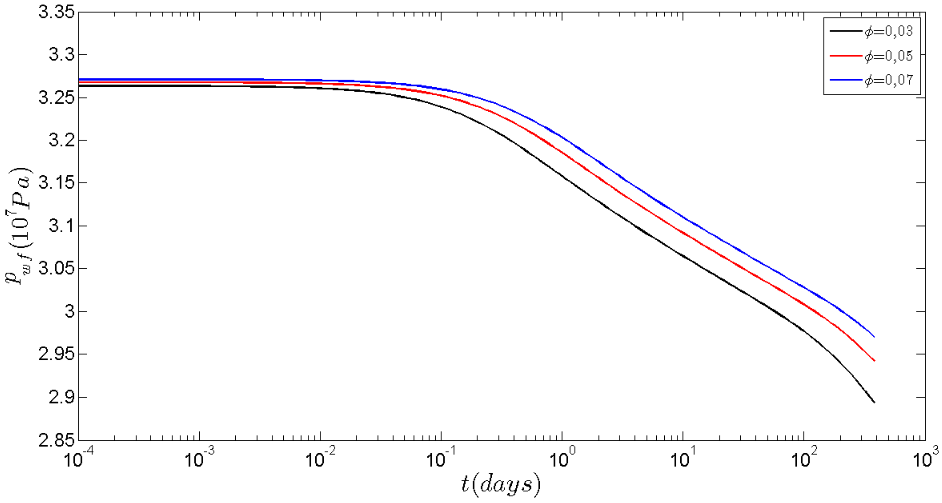

Figure 8: Results for different porosities.

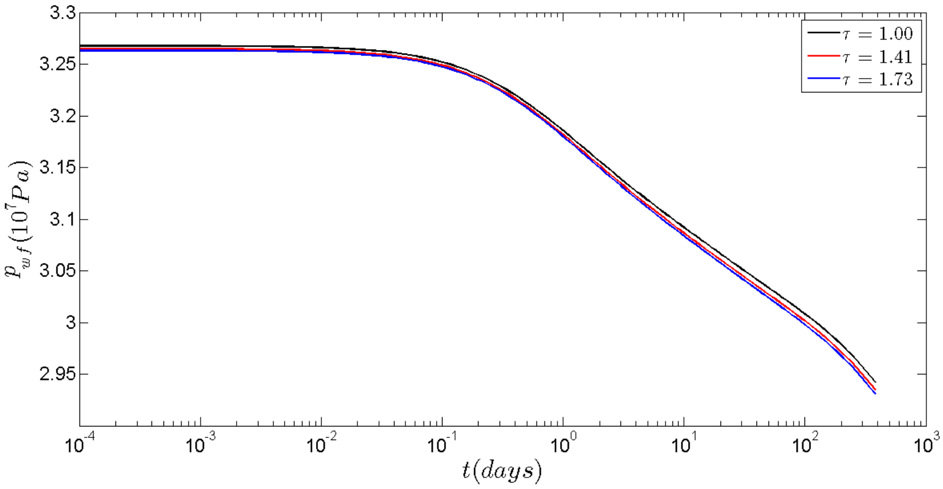

Figure 9: Results for different rock tortuosities.

Finally, more two important parameters for Knudsen's number and for the porous media flow were tested. Figs. 10 and 11 show results for variations in specific gas gravity, γ_g, and in temperature, respectively. For specific gas gravity we have $\gamma_g = M/M_{air}$, where M_{air} is the molecular weight for air. Variations in γ_g influences correctly perception of the reservoir boundaries (earlier for lower γ_g). The effect in Δp for Kn analysis is also adequate and the same is obtained for temperature (increments in T increase Kn).

5 CONCLUSIONS

In this paper, we applied a modified Darcy's law to take in account non-Darcy's flow due to slippage effect, in order to simulate numerically flow in shale gas reservoirs. Finite-difference

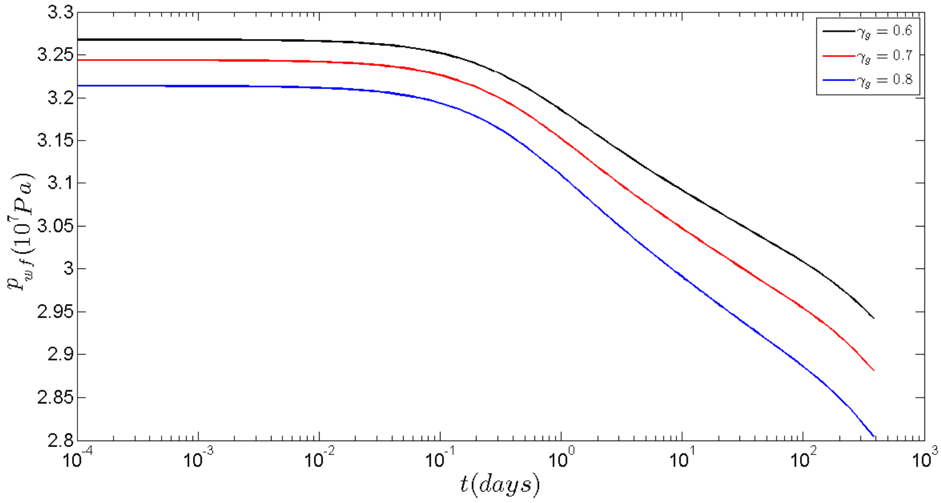

Figure 10: Results for different specific gas gravities.

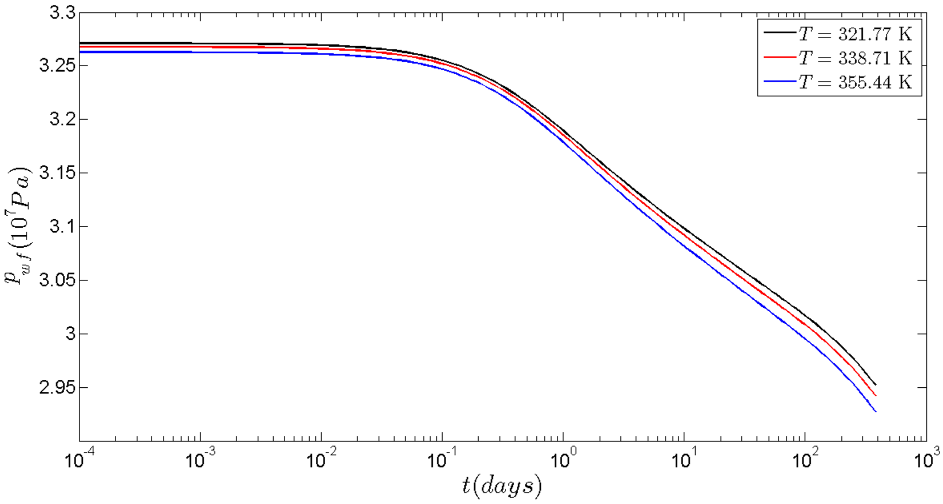

Figure 11: Results for different temperatures.

method and an implicit formulation were used in order to obtain numerical solution for the wellbore pressure for a constant production rate, in a model of field scale and for production through horizontal well. The correction used for apparent permeability is a Knudsen's number function. Comparing solutions from Darcy's law and from slippage model it was possible to note significant differences between the pressure drop curves and to give us insights as to how parameters like ϕ, γ, T and k_∞ influence the results. The methodology employed was able to detect slip effects. Indeed, analysis of the results indicated that a careful study should be conducted for numerical reservoir simulation and reservoir characterization. It is very important to note that parameters tested for Kn also influences the global flow behavior, in way that the pressure drop changes must be discussed envolving two contexts: conventional Darcy's law for viscous flow and Knudsen's number for slippage phenomena. As example, for intrinsic permeability, a lower value increases pressure drop. But it also increases Kn, increasing apparent permeability, reducing pressure drop. This type of balance exists for other parameters in the modeling

ACKNOWLEDGMENTS

Authors gratefully thanks Universidade do Estado do Rio de Janeiro, CAPES and CNPq for their support.

REFERENCES

Akgun, F., 2004. A finite element model for analyzing horizontal well BHA behavior. *Journal of Petroleum Science and Engineering*, vol. 42, No. 1-2, pp. 121–132.

Al-Mohannadi, N. S., 2004. *Simulation of Horizontal Well Tests*. PhD Thesis, Colorado School of Mines/Golden.

Al-Mohannadi, N.S., Ozkan, E. & Kazemi, H., 2007. Pressure-transient responses of horizontal and curved wells in anticlines and domes. *Society of Petroleum Engineers Reservoir Evaluation & Engineering*, vol. 10, n. 1, pp. 66–76.

Aziz, K. & Settari, A., 1979. *Petroleum Reservoir Simulation*. Applied Science Publishers LTD., England.

Bestok, A. & Karniadakis, G. E., 1999. A Model for Flows in Channels, Pipes, ans Ducts at Micro and Nano Scales. *Microscale Thermophysical Engineering*, vol. 3, pp. 43–77.

Bird, R. B., Stewart, W. E. & Lightfoot, E. N., 2002. *Transport Phenomena*. Second Edition, John Wiley & Sons, Inc., USA.

Chastanet, J., Royer, P. & Auriault, J.-L., 2007. Flow of low pressure gas through dual-porosity media. *Transport in Porous Media*, vol. 66, n. 1, pp. 457–479.

Chaudhry, A. U., 2003. *Gas Well Testing Handbook*. Elsevier, Burlington, Massachusetts, USA.

Civan, F., 2010 a. Effective Correlation of Apparent Gas Permeability in Tight Porous Media. *Transport in Porous Media*, vol. 82, n. 1, pp. 375–384.

Civan, F., 2010 b. Non-isothermal Permeability Impairment by Fines Migration and Deposition in Porous Media including Dispersive Transport. *Transport in Porous Media*, vol. 85, n. 1, pp. 233–258.

Civan, F., Chandra, S. R. & Sondergeld, C. H., 2011. Shale-Gas Permeability and Diffusivity Inferred by Improved Formulation of Relevant Retention and Transport Mechanisms. *Transport in Porous Media*, vol. 86, n. 1, pp. 925–944.

Computational Modeling Group, 2009. *IMEX, Advanced Oil/Gas Reservoir Simulator*. Computational Modeling Group.

De Souza, G., 2013. *Acoplamento Poço-reservatório na Simulação Numérica de Reservatórios de Gás*. PhD Thesis, Universidade Estadual do Norte Fluminense/Macaé.

De Souza, G., Pires, A.P. and Abreu, E., 2014. Well-reservoir coupling on the numerical simulation of horizontal wells in gas reservoirs. *In Society of Petroleum Engineers Latin America and Caribbean Petroleum Engineering Conference.*, 21–23 May, Maracaibo, Venezuela.

Dranchuk, P. M. & Abou-Kassem, J. H., 1975. Calculation of Z factors for Natural Gases using Equations of State. *Journal of Canadian Petroleum Technology*, vol. 14, n. 3, pp. 34–36.

Dumkwu, F. A., Islam, A.W., & Carlson, E. S., 2012. Review of Well Models and Assessment of their Impacts on Numerical Reservoir Simulation Performance. *Journal of Petroleum Science and Engineering*, vols. 82-83, pp. 174–186.

Ertekin, T., Abou-Kassem, J. H., & King, G. R., 2001. *Basic Applied Reservoir Simulation*. Society of Petroleum Engineers.

Florence, F. A., Rushing, J. A, Newsham, K. E. & Blasingame, T. A., 2007. Improved Permeability Prediction Relations for Low Permeability Sands. *Society of Petroleum Engineers Rock Mountain Oil & Gas Technology Symposium*, 16–18 April, Denver, Colorado, USA.

Hayek, M., 2015. Exact Solutions for One-Dimensional Transient Gas Flow in Porous Media with Gravity and Klinkenberg Effects. *Transport in Porous Media*, vol. 107, n. 1, pp. 403–417.

He, J. & Durlofsky, L. J., 2013. Reduced-order Modeling for Compositional Simulation Using Trajectory Piecewise Linearization. *Society of Petroleum Engineers Reservoir Simulation Symposium*, 18-20 February, The Woodlands, Texas, USA.

Hu, G., Wang, H., Fan, X., Yuan, Z. & Hong, S., 2009. Mathematical Model of Coalbed Gas Flow with Klinkenberg Effects in Multi-Physical Fields and its Analytic Solution. *Transport in Porous Media*, vol. 76, n. 1, pp. 407–420.

Jmili, A., Wilhite, G. P., & Green, D., 2011. Modeling Gas-phase Mass Transfer Between Fracture and Matrix in Naturally Fractured Reservoirs. *Society of Petroleum Engineers Journal*, vol. 16, n. 4, pp. 795–811.

Lee, A. L., Gonzalez, M. H., & Eakin, B. E., 1966. The Viscosity of Natural Gases. *Petroleum Technology, Transactions of AIME*, vol. 18, n. 8, pp. 997–1000.

Li, D., Xu, C., Wang, J. Y. & Lu, D., 2014. Effect of Knudsen diffusion and Langmuir adsorption on pressure transient response in tight- and shale-gas reservoirs. *Journal of Petroleum Science and Engineering*, vol. 124, pp. 146–154.

Peaceman, D. W., 1983. Interpretation of Well-block Pressures in Numerical Reservoir Simulation with Nonsquare Grid Blocks and Anisotropic Permeability. *Society of Petroleum Engineers Journal*, vol. 23, n. 3, pp. 531–543.

Saad, Y., 2003. *Iterative Methods for Sparse Linear Systems*. Second edition. Society of Industrial and Applied Mathematics, Burlington, USA.

Shahbazi, S., Maarefvand, P. and Gerami, S., 2015. Investigation on flow regimes and non-Darcy effect in pressure test analysis of horizontal gas wells. *Journal of Petroleum Science and Engineering*, vol. 129, pp. 121–129.

Swami, V., Clarkson, C. R. & Settari, A., 2012. Non Darcy Flow in Shale Nanopores: Do We Have a Final Answer? *Society of Petroleum Engineers Canadian Unconventional Resources Conference*, 30 October-1 November, Calgary, Alberta, Canada.

Tiab, D. & Donaldson, E. C., 2004. *Petrophysics, Theory and Practice of Measuring Reservoir Rock and Fluid Transport Properties*. Gulf Professional Publishing.

Wu, Y.-S. & Fakcharoenphol, P., 2011. A Unified Mathematical Model for Unconventional Reservoir Simulation. *Society of Petroleum Engineers EUROPEC/EAGE Annual Conference and Exhibition*, 23-26 May, Vienna, Austria.

Wu, Y.-S., Pruess, K. & Persoff, Persoff, 1998. Gas Flow in Porous Media with Klinkenberg Effects. *Transport in Porous Media*, vol. 32, n. 1, pp. 117–137.

Xie, W., Li, X., Zhang, L., Wang, J., Cao, L. and Yuan, L., 2014. Two-phase pressure transient analysis for multi-stage fractured horizontal well in shale gas reservoirs. *Journal of Natural Gas Science and Engineering*, vol. 21, pp. 691–699.

Ziarani, A. S. & Aguilera, R., 2012. Knudsen's Permeability Correction for Tight Porous Media. *Transport in Porous Media*, vol. 91, n. 1, pp. 239–260.